JOURNAL OF GEOPHYSICAL RESEARCH, VOL. 97, NO. E8, PAGES 13,601–13,610, AUGUST 25, 1992

Joints in Venusian Lava Flows

CATHERINE L. JOHNSON AND DAVID T. SANDWELL

Scripps Institution of Oceanography, La Jolla, California

Venusian plains regions, as imaged by the Magellan spacecraft, display many styles of tectonic and volcanic deformation. Radar images of several areas of the volcanic plains reveal polygonal patterns of bright lineations. Intersection geometries of the lineations defining the polygonal patterns are typical of those found in tensile networks. In addition, the polygonal patterns generally exhibit no preferred orientation, implying that they are the result of horizontally isotropic stress fields. Such stress fields usually arise on the Earth as a consequence of desiccation, freeze-thaw cycles, or cooling and produce mud cracks, ice-wedge polygons, and columnar joints, respectively. We propose that the polygonal patterns seen in the Magellan images of some of the volcanic plains are the result of thermal stresses. We consider two alternative scenarios which would generate sufficient tensile thermal stresses to cause failure. The first scenario is that of a cooling lava flow; the residual thermal stress which would develop (assuming no failure of the rock) is tensional and of the order of 400 MPa. This is much greater than the strength of unfractured terrestrial basalt (~10 MPa), so we can expect joints to form during cooling of Venusian lava flows. However, the spacing of the polygonal lineations seen in Magellan images is typically 1-2 km, much larger than the largest spacings of decimeters for joints in terrestrial lavas. The second scenario involves an increased heat flux to the base of the lithosphere; the resulting thermal stresses cause the upper lithosphere to be in tension and the lower lithosphere to be in compression. Brittle tensile failure occurs near the surface due to the finite yield strength of the lithosphere. The maximum depth to which failure occurs increases with increasing elevation of the temperature gradient. For an initially 25-km-thick lithosphere and temperature gradient of 11°/km, this maximum depth varies from 0.5 km to 2 km as the temperature gradient is increased to 12°/km and 22°/km, respectively. Both the cooling flow scenario and the heated lithosphere scenario produce isotropic tensile surface stress patterns, but the heated lithosphere model is more compatible with the kilometer scale of the polygonal patterns seen in Magellan images.

INTRODUCTION

Radar images obtained from the Magellan spacecraft reveal extensive plains displaying both tectonic and volcanic deformation. Some plains terrains are smooth and featureless, some show lobate areas of differing radar brightness, and some display radar-bright lineations of compressional and/or extensional origin [*Saunders et al.*, 1991]. Radar-bright lineaments identifiable as graben may extend for hundreds of kilometers. Other bright sinuous features are compressional in origin and similar to 'wrinkle' ridges seen on the moon. Some plains display intersecting sinuous features which are not identifiable as compressional or extensional. In several areas (Figure 1), intersecting bright lineations form polygonal patterns (Figure 2), which resemble fracture networks often developed in terrestrial rocks and soils.

Polygonal fracture networks on Earth commonly result from desiccation (e.g., mud cracks), freeze-thaw cycles (e.g., ice-wedge polygons), or cooling (e.g., columnar joints). Such fracture networks are usually dominated by tetragonal, pentagonal, and hexagonal polygons [*Peck and Minakami*, 1968; *Ryan and Sammis*, 1978; *Aydin and DeGraff*, 1988]. Although the surface pattern of two types of shrinkage cracks may be the same, the ratio of the horizontal crack spacing to the crack depth may be different. For example, it can be observed that the ratio of crack spacing to crack depth for mud cracks is usually much greater than one, whereas for joints in terrestrial lava flows it is much less than one. On Venus, the surface conditions prohibit dessication or freeze-thaw cycles as causes of the polygonal fracture patterns. However, extensive lava flows and many volcanic edifices are evident, supporting the possibility that the polygonal patterns may be of thermal origin.

On Earth, columnar jointing in lava flows and sills is common, e.g., the Giants Causeway in Northern Ireland, the Columbia River Basalts, and the lava lakes in Hawaii. Such jointing is the result of thermal stresses which develop as the lava cools and solidifies. Extensive research has been done, examining the evolution of polygonal joint patterns [*Aydin and DeGraff*, 1988], the relationship of jointing structures to cooling history [*Long and Wood*, 1986], observations of joint formation in Hawaiian lava lakes [*Peck and Minakami*, 1968], the mechanics of joint growth from observations of small-scale structures on joint faces [*DeGraff and Aydin*, 1987] and the relationship of joint spacing to cooling rate and joint growth increment [*DeGraff and Aydin*, 1986]. The processes of joint formation, interaction, propagation, and arrest are not yet well understood, but substantial progress has been made over the last 15 years [*Nemat-Nasser et al.*, 1978; *Keer et al.*, 1978; *Nemat-Nasser et al.*, 1980].

On the basis of morphology, we propose that the bright polygonal patterns seen in some Magellan images of the volcanic plains are joint networks. We identify several areas displaying such patterns, noting their areal extent, the presence of volcanic features, and the regional topography. One area with well-developed polygonal patterns is described in detail, presenting evidence to suggest the patterns are tensional networks. We demonstrate that sufficient tensile stresses develop in a cooling Venusian flow to allow joints to form and that the thermal strain predicted is not incompatible with that observed. The major difference between the polygonal fracture patterns seen in the Magellan data and joints in terrestrial lavas is one of scale. The spacing of the Venusian features is of the order of kilometers,

Paper number 92JE01212.
0148-0227/92/92JE-01212$05.00

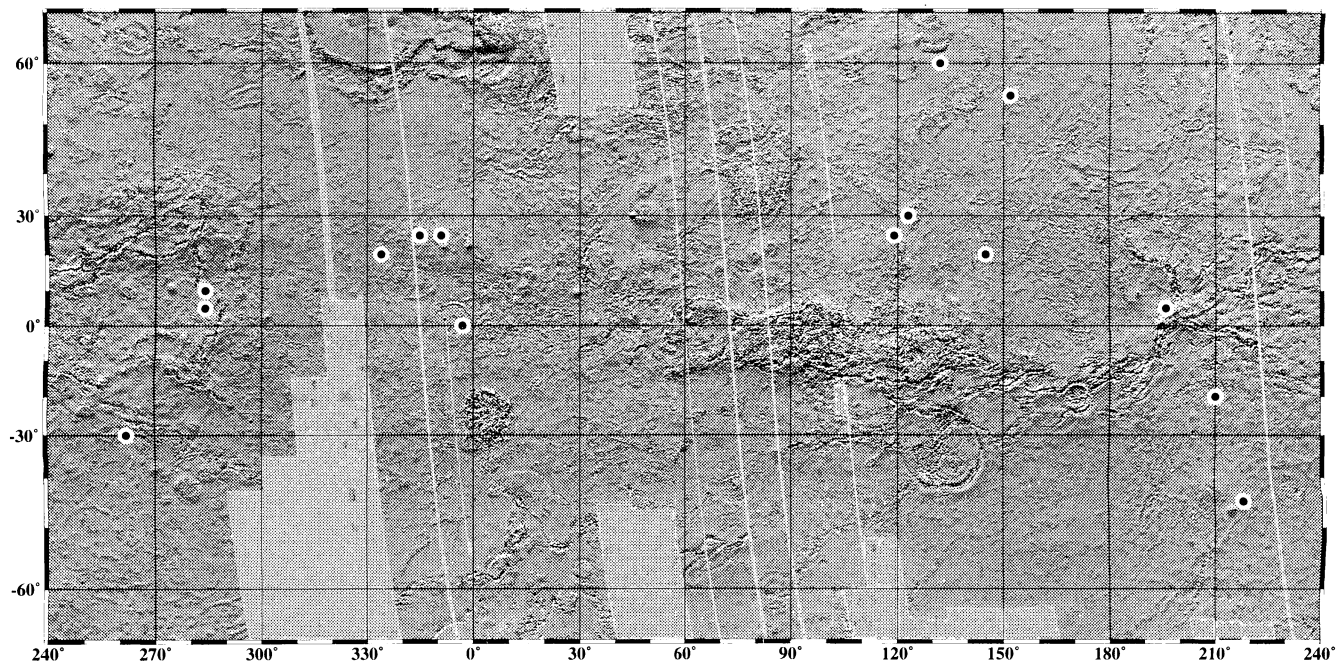

Fig. 1. Mercator projection [*Ford and Pettengill*, this issue] map of Venus. Illumination is from the north along altimeter orbits; thus grey shade represents topographic slope. Dots indicate areas identified in the high-resolution Magellan synthetic aperture radar images as exhibiting polygonal patterns. Areas which overlap two adjacent images are shown as one dot only. All areas lie within 1 km of the mean planetary radius for Venus (6051.9 km) but appear to be randomly distributed and uncorrelated with particular geographical features.

whereas the spacing of joints in terrestrial lavas varies from decimeters to centimeters. Factors which may cause such a difference in scale are discussed. It is possible that the tensional networks are the result of a thermally stressed layer much thicker than a single lava flow. We consider a second model in which thermal stresses develop as a result of regional elevation of the temperature gradient. In this case a layer up to a few kilometers thick undergoes brittle tensile failure.

DATA ANALYSIS

A preliminary analysis of Magellan synthetic aperture radar (SAR) and altimeter data has revealed 15 areas displaying bright polygonal patterns (Figure 1). If the polygonal patterns are tensional fracture networks, resulting from the cooling and contraction of lava flows, then the fracture patterns should occur in areas that have been resurfaced by lava flows (identify flow source(s) and extent) and the edges of the fracture patterns should correlate with the margins of the flows. Alternatively, if the polygonal patterns are the result of thermal stresses in a thicker layer (upper crust or lithosphere), the edge of the patterns will not necessarily correlate with the limits of a lava flow. Below we discuss one area in detail, presenting evidence to support the hypothesis of a thermal contraction origin for the polygonal patterns.

The area which we have selected for detailed discussion is a region southeast of Nightingale Corona, at ~60°N, 135°E (Figure 2) as polygonal patterns are clearly identifiable and are not obscured by contemporaneous or later volcanism/tectonism. The edge of the corona is seen as a bright feature in the top left of the image and is associated with a flexural signature in the topography [*Johnson and Sandwell*, 1992]. Aside from this flexure, the region is extremely flat with regional slopes of < 1°. Figure 3 shows Magellan topography profiles [*Ford and Pettengill*, this issue] along sections XX', YY', ZZ' of Figure 2. Bright polygonal patterns are evident on the dark plains. Possible origins for such smooth (radar-dark) flat areas include resurfacing by extremely fluid lavas (analogous to terrestrial flood basalts) ash cover or tuffs. It is evident from thin mantling deposits identified in some areas that pyroclastic eruptions do occur on Venus [*Guest and Bulmer*, 1992]. However, it is currently believed that this type of eruption is unlikely to occur under Venusian conditions unless the volatile content of the ascending magma is in the range 2-4%; when pyroclastic eruptions do occur, the pyroclasts themselves will be much less widely distributed than on Earth [*Head and Wilson*, 1986]. It is thus more likely that the dark background in the radar image is the result of lava flow(s) rather than ash cover or nuee ardente type flows. Although difficult to discern in Figure 2, the edge of the polygonal patterns (very southern part of the image) appears to coincide with a boundary between areas of slightly different radar brightness. We propose this is the edge of one or more lava flows. Smaller, brighter flows occur closer to the corona edge and are easily identified by their lobate forms (FMIDR_ 60N132, Jet Propulsion Laboratory). Lava flows and other volcanic features are commonly seen in and around coronae on Venus [*Stofan et al.*, this issue]. It is therefore feasible that the extensive flows to the southeast of Nightingale are associated with the corona. The radial lineations which terminate at the edge of the corona and are distinguishable as depressions may be dikes, possible feeders for volcanic flows.

Polygonal patterns over the eastern part of the area are shown at higher resolution in Figure 4. The intersections of the bright lineations defining the polygons show geometries identical to those of shrinkage cracks on Earth: T intersections, curved-T intersections, and Y intersections [*Aydin and DeGraff*, 1988]. Examples of these intersection types are shown in Figure 4 with

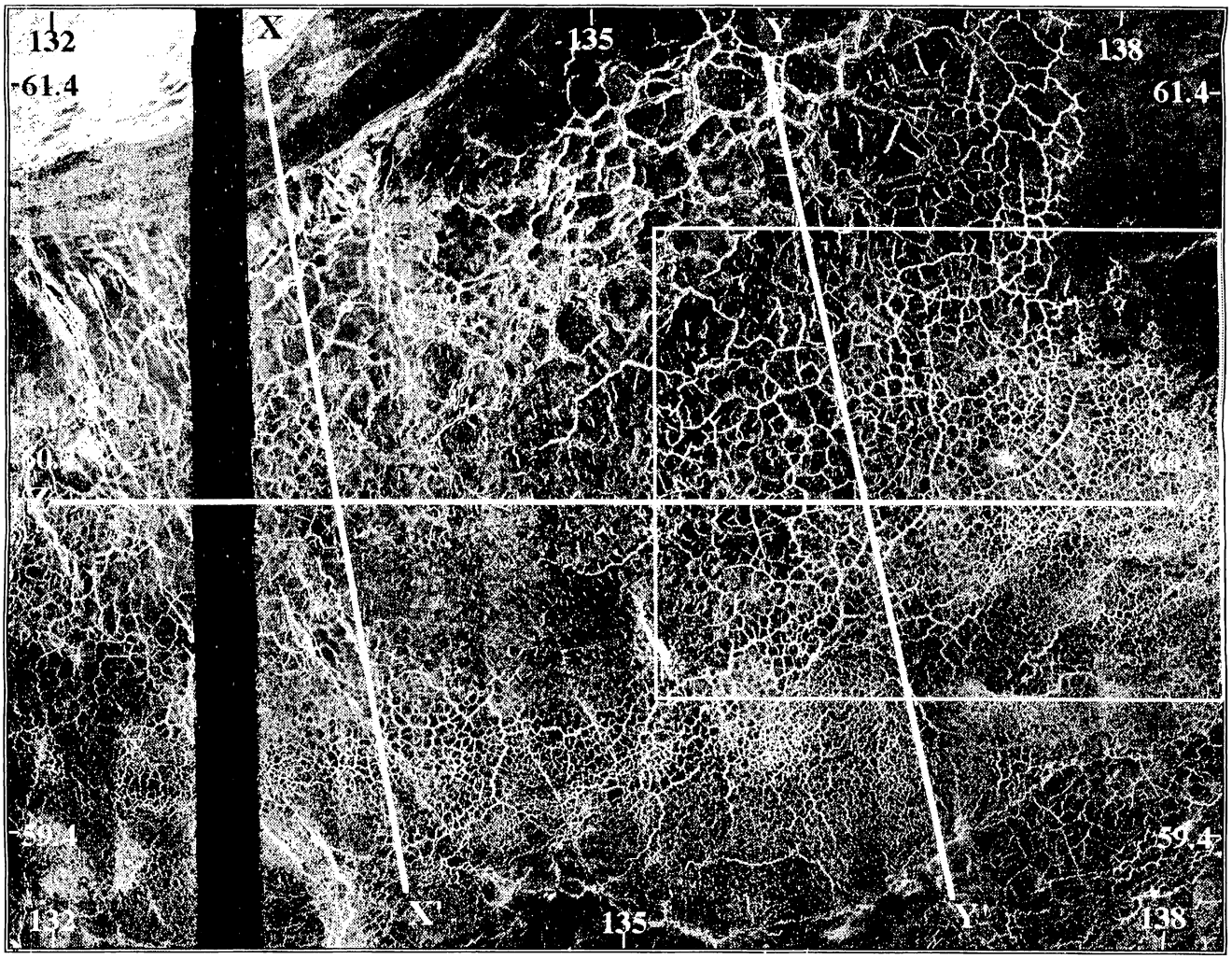

Fig. 2. Portion of Jet Propulsion Laboratory Magellan image F-MIDR.60N132 (look direction is left) showing part of the Venusian plains southeast of Nightingale Corona. The edge of the corona can be seen in the upper left corner of the image. The area is about 350 km in longitude by 270 km in latitude. Altimetry profiles along XX', YY', ZZ' are shown in Figure 3. The boxed region in the eastern part of the image is shown in more detail in Figure 4.

interpretation sketches alongside the image. On Earth, the order of joint formation at T and curved-T intersections is through joint first followed by the truncated joint, as the later joint cannot propagate across an existing fracture. Such T and curved-T intersections are common at the surface of terrestrial lava lakes where joints form sequentially [*Aydin and DeGraff*, 1988]. Examples A and B (Figure 4) show such a geometry: one bright lineation is truncated against another continuous lineation. Y-type intersections may result from three joints initiating at a common weak point in the material, from branching of a propagating joint, or from joints growing toward one another. Example C (Figure 4) is typical of a Y intersection, although it is not possible to distinguish by which of the above mechanisms it was formed. Example D may represent an early stage in the formation of Y intersection. Here three bright lineations of similar lengths terminate just short of a common intersection point. Few Y intersections are present (Figures 2 and 4). This is consistent with observations of terrestrial flows, where Y intersections are more common in the interior of a flow than at the surface [*Aydin and DeGraff*, 1988]. In cases where terrestrial joints approach one another they curve away from each other and form overlappers. Examples E and F (Figure 4) are typical of such overlappers.

The variation in mean spacing of the lineaments (polygon widths) in the area (Figures 2 and 4) was made by estimating the average spacing of these lineaments on lines taken at varying orientations across different parts of the region. Although crude, this method provides a sufficiently accurate result for the purpose of this study. Mean spacings range from 1-2 km (southern portion of the area) to 8 km (close to the corona edge). An interesting observation is that the wider polygons are associated with the edge of the topographic flexural signature around the corona. The smaller polygons occur where the topography is extremely flat. The width of the lineations themselves range from less than the resolution of one pixel (75 m) in the southern portion of the image, to 500 m close to Nightingale Corona. The lower limit on lineation width is not known as a topographic feature significantly narrower than 75 m may be detected by the SAR if the energy returned from the feature is substantially more than that returned from the immediately surrounding terrain. An obvious feature of the polygonal patterns in Figure 2 is that narrower lineations are associated with smaller polygons.

We have proposed above that the plains to the southeast of Nightingale Corona are the result of extensive lava flows, probably associated with the corona itself. Unfortunately, most of the

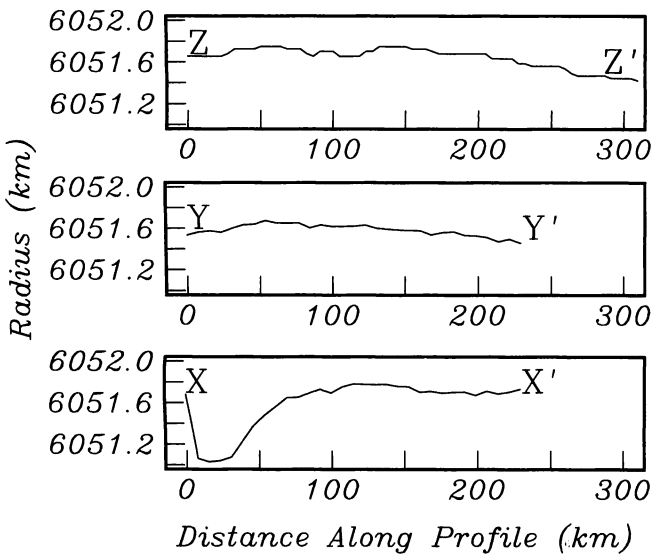

Fig. 3. Magellan altimetry profiles XX', YY', ZZ' as indicated in Figure 1. Profile XX' is along orbit 1232. The topographic low outboard of Nightingale Corona can be seen between 10 km and 30 km along the profile. Beyond 100 km the topography is extremely flat. Profile YY' is along orbit 1246. Profile ZZ' was taken from the gridded altimetry [*Ford and Pettengill*, this issue] along a line of latitude. The regional slope is < 1° downhill to the southeast.

lineations comprising the bright polygonal patterns associated with the flow(s) are too narrow to be distinguishable as ridges or depressions. However, close to the corona edge a few wider lineations are just discernable as depressions: the more westerly side of the lineation is dark compared with the more easterly side. Intersection geometries of the lineations comprising the polygonal patterns are typical of the geometries found in tensional networks. We do not believe the patterns seen here are the result of regional tectonic stress fields because they are isotropic. The observations and arguments above strongly support the hypothesis that these polygonal patterns are analogous to joint networks found in terrestrial lava flows.

For seven of the 15 areas shown in Figure 1 the flow source(s)/extent could be identified, and the edge of the area of polygonal patterns was seen to correlate with the edge of the lava flow(s). The major characteristics of these seven areas are summarized in Table 1. Polygon and lineament widths were measured for each area as described above. It can be seen that the the smaller polygon widths (1-3 km) and lineament widths (< 75-150 m) in the polygonal patterns around Nightingale Corona are typical of those identified in other areas, but the larger-scale patterns at Nightingale are not observed elsewhere. All the areas identified in Table 1 are extremely flat (slopes < 1°) and lie at elevations between ± 1 km of the mean planetary radius (6051.9 km). This is not particularly suprising as most of the highland regions on Venus are extremely tectonically deformed. Lakshmi Planum is the only extensive upland area which has low topographic relief and a smooth radar-dark surface, but it does not display polygonal networks. In five regions, clusters of small shield volcanoes were present, further evidence that the regions exhibiting polygonal networks are associated with substantial volcanic activity. Possible collapsed lava tubes are present in the corona centered at 31.5°S, 259.5°E, coincident with an area displaying polygonal networks (Table 1). In some regions, tectonic and/or volcanic processes postdate the formation of the polygonal patterns. Such an example occurs in part of Guinevere Planitia; part of this area is shown in Figure 5. The polygonal patterns can be seen, but later tectonic deformation has resulted in

TABLE 1. Major Characteristics of the Seven Areas Shown in Figure 1

FMIDR	Areal Extent, km	Mean Radius, km	Fracture Spacings, km	Fracture Widths, m	Comments
F45S 218 (46.5S, 219.0E)	110 (E-W) 110 (N-S)	6052.5	1-2	<= 75	Flows associated with large volcano in Imor Regio to SW. Several small shield volcanos. Some N-S compressional ridges. Later flows obscure some of polygonal patterns.
F30S262 (31.4S, 259.2E)	100 (E-W) 80 (N-S)	6051.5	1-3	< 75-150	Polygonal patterns associated with flows within corona. Several shield volcanoes. Possible collapsed lava tubes at (31.6°S, 259.8°E), (31.2°S,260.3°E).
F20S210 (20.0S, 211.3)	a) 80 (E-W) 70 (N-S)	6051.9	1-3	< 75-150	Area is NW of larger of two coronae in image SW-NE trending lineations postdate polygonal patterns. Many small shields and some compressional ridges.
	b) 30 (E-W) 40 (N-S)	6051.1	1-3	< 75-150	Area is within the smaller corona.
F05N195 (6.6N, 192.5E)	200 (E-W) 200 (N-S)	6052.7	1-2	<= 75	Area in east Russalka Planitia just north of bright flows from Maat Mons. A few small shield volcanoes. "Wrinkle" ridges along eastern edge region polygonal patterns.
F10N284 (7.9N, 282.9E)	25 (E-W) 25 (N-S)	6050.7	0.5-1.5	< 75-150	Several small patches at south end of Devana Chasma. Two easily distinguished ones identified here. Extensive tectonic deformation.
(10.5N, 283.9E)	25 (E-W) 25 (N-S)	6050.4	0.5-1.5	< 75-150	
F20N334 (21.0N, 334.0E)	220 (E-W) 300 (N-S)	6050.7	1-2	< 75-150	Small shield volcanoes and N-S and NW-SE bright lineations appear to postdate polygonal patterns. Polygonal networks extend into F25N333.
F60N132 (60.5N, 137.0E)	330 (E-W)	6051.6	1-8	< 75-500	Area to SE of Nightingale Corona. Larger-scale polygons coincide with flexure in topography. Smaller-scale polygons in flat region south of flexure.

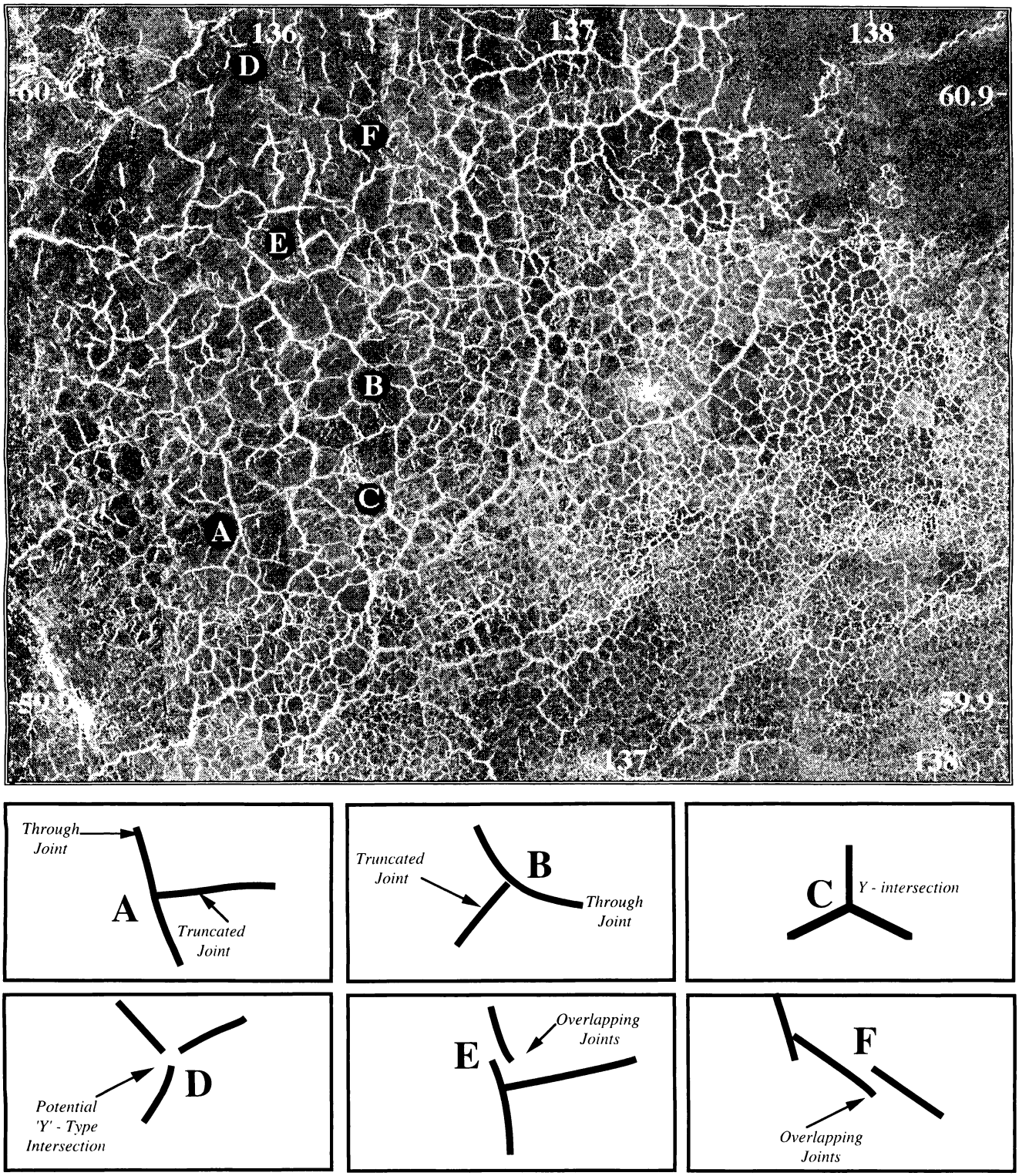

Fig. 4. Boxed region in figure 2 is shown in more detail. Points marked A (60.2°N, 135.8°E), B (60.4°N, 136.2°E), C (60.2°N, 136.3°E), D (61.0°N, 135.8°N), E (60.7°N, 136.0°E), and F (60.8°N, 136.3°E) are referred to in the text and correspond to the labeled interpretation sketches alongside the SAR image. Interpretations A, B, and C indicate T-type, curved-T-type, and Y-type joint intersection geometries characteristic of terrrestrial jointing. D corresponds to a possible early stage of evolution of a terrestrial Y-type intersection. E and F show bright lineations which are analogous to overlapping joints or echelon cracks on Earth.

closely spaced (~1 km) N-S and NW-SE trending bright lineations. The shield volcano in the center of the image is one of many in the region and appears to postdate both the polygonal patterns and the later lineations. In portions of this area there appears to be some orientation to the polygonal patterns, with lineations being preferentially aligned along and perpendicular to the regional topographic gradient (< 1°, downhill to the SW).

In summary, 15 regions have so far been identified as

displaying polygonal patterns in the Magellan SAR images. Seven of these areas can be identified as regions of extensive lava flow(s), where the limits of the lava flow(s) correlate well with the spatial extent of the polygonal patterns. Furthermore, the polygonal patterns are identified as tensional and probably unrelated to local and regional tectonics due to their lack of preferred orientation.

DISCUSSION

We have presented observational evidence supporting the idea that polygonal patterns seen in Magellan SAR images are tensional networks. Spatial correlation of the patterns with volcanic flows, the isotropic nature of the patterns and the joint intersection geometries described in detail above suggest an analogy with terrestrial lava flow joints in seven areas. In the remaining eight areas, correlation of the edge of the patterns with flow limits is poor, but the patterns are still associated with extensive volcanism. The major difference between terrestrial joints and the tensional networks seen in the Magellan data is the width of the polygons (joint spacing) and the lineations defining them (joint width). On Earth, joints in lava flows have typical spacings of decimeters to a meter and widths of a few centimeters [e.g., *Peck and Minakami,* 1968]. The Venusian features typically have spacings of 1-2 km and widths of less than 75-150 m (i.e., less than 2 pixels). In this section we consider possible origins for the Venusian polygonal patterns. If the patterns are directly analogous to terrestrial joints, then sufficient thermal stresses must be generated in a cooling flow to cause tensile failure of the rock, the predicted thermal strain must be compatible with that observed, and the difference in scale between the Venusian patterns and columnar joints on the Earth must be explained. Alternatively, the patterns may be the result of thermal stresses generated in the upper crust/lithosphere rather than in a single lava flow. If this is so, the mechanism producing the thermal stress must be investigated and an estimate of the yield strength envelope for the Venusian lithosphere is needed to determine whether failure would occur for a given thermal stress profile. These issues are discussed in detail below.

In an ideal case, a cooling lava flow solidifies but cannot retain any thermal stress until it cools through an elastic "blocking temperature"; below this temperature, elastic stresses accumulate according to

$$\sigma_{xx}(z,t) = \alpha * \frac{E}{1-\nu} * \Delta T(z,t) \qquad (1)$$

where

$$\Delta T(z,t) = T(z,t) - T_e$$

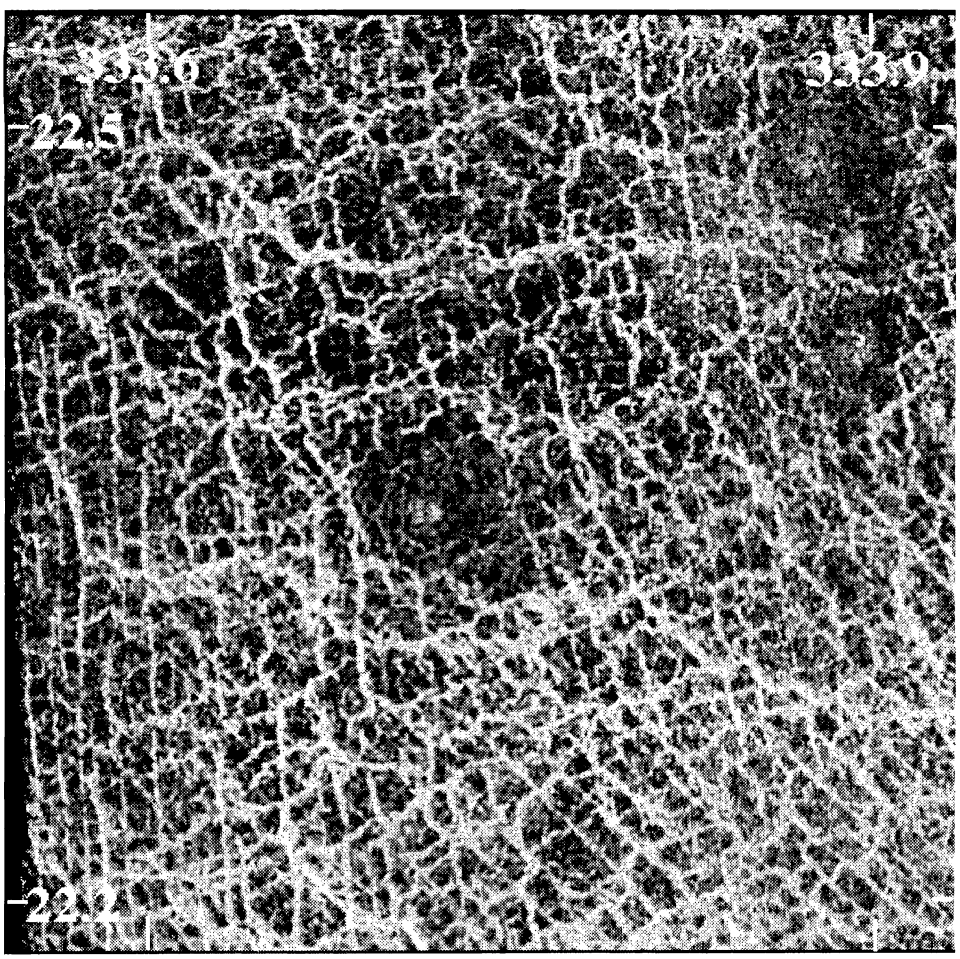

Fig. 5. Portion of JPL MIDR.20N334 (look direction is left). Image is 39 km (E-W) by 38 km (N-S). The polygonal patterns are overlain by two sets of parallel bright lineations spaced at ~1 km; one set trending N-S, the other NW-SE. Several shield volcanoes are present, the most prominent of which is centered at 22.35°N, 333.70°E. The shield volcanoes appear to postdate both the polygonal patterns and the later lineations. The tectonic and volcanic deformation postdating the polygonal networks renders detailed analysis of polygon spacing and width difficult.

[*Boley and Weiner*, 1960; *Parmentier and Haxby*, 1986]. T_e is the elastic blocking temperature, α is the coefficient of linear thermal expansion, E is Young's modulus, and υ is Poisson's ratio. We use terrestrial values of 10^{-5} °C^{-1} for α, 7×10^{10} N m^{-2} for E, and 0.25 for υ.

Joints have been observed to initiate in Hawaiian lava lakes at temperatures between 900°C and 980°C [*Peck and Minakami*, 1968]. Assuming a similar blocking temperature range for Venusian lavas and no failure of the rock, residual tensional stresses of the order of 400 MPa are predicted. This greatly exceeds the tensile strength of unfractured terrestrial basalt (~10 MPa) [*Peck and Minakami*, 1968]. Thus, if Venusian lavas are of comparable strength to terrestrial basalts, the thermal stresses generated in a cooling flow will cause the flow to fail in tension from the top surface downward and the bottom surface upward. This is exactly how joints form in terrestrial flows [*Peck and Minakami*, 1968; *Ryan and Sammis*, 1978; *DeGraff and Aydin*, 1988; *Pollard and Aydin*, 1988].

The thermal strain generated in a cooling flow is equal to $\alpha\Delta T$ l, where l is the joint spacing. For a joint spacing of the order of 1 km, we would expect the final joint width to be ~5 m. As seen in Figure 2, the widths of individual fractures seems to increase as the spacings of the fractures increases. Fracture spacings of the order of 1 km are generally associated with fractures that are less than or equal to the pixel spacing (75 m). However, a linear feature less than 75 m can be detected by the SAR, as long as the energy return from the feature is much greater than the radar return from the surrounding terrain [*Sabins* 1978; N. Izenberg and R. Brackett, personal communication, 1992]. Although comparison with terrestrial joints would suggest that we would not expect significant widening of a tensional crack by weathering, we need to remember that the features seen in the Venusian images are much wider than terrestrial joints which could lead to some failure and slumping, thus increasing the width of the feature at the surface.

The arguments above indicate that the thermal stresses generated in a cooling lava flow under Venusian surface conditions exceed the (terrestrial) tensile strength of the rock and that the thermal strain predicted may be compatible with that observed in the SAR images. If the tensional networks are lava flow joint networks, we need to explain the major difference in scales between the Venusian features (~10^3 m) and terrestrial columnar joints (~1 m); this is hampered by the fact that there is currently no simple physical model for the typical widths and spacings of joints on Earth. We next consider factors which might cause joints on Venus to be much more widely spaced than on Earth.

On Earth a relationship between lava flow joint spacing and cooling rate is observed: polygon widths are generally greater at the base of a flow than at the top, due to the relatively slower cooling of the base [*James*, 1920; *Spry*, 1962; *Pollard and Aydin*, 1988]. Where quenching of a flow by rainfall has occurred, joints are more closely spaced, and in extreme cases the regular columnar structure may be replaced a more irregular pattern of joints known as an entablature structure [*Long and Wood*, 1986]. On Venus, the high surface temperature means that the cooling rate of a flow will be lower than on Earth. Also the absence of water on the surface of Venus means that cooling of a flow will be entirely by conduction as compared with terrestrial flows where cooling is often accelerated due to convective cooling following flooding events. We would therefore expect Venusian joints to be spaced somewhat wider than at the upper surface of terrestrial flows; however, a 500-fold increase does not seem plausible. It should also be noted that the thermomechanical properties of a "dry" basalt at Venusian surface conditions are not known. It is possible that lava flows on Venus may be stronger than their terrestrial counterparts, although what effect this would have on joint spacing is not clear.

No dependence of joint spacing on lava flow thickness is observed for terrestrial lava flows; joints initiate before the flow has completely solidified [*Peck and Minakami*, 1968]. *Head and Wilson* [1992] suggest that magma reservoirs may be larger on Venus than on Earth which could give rise to either thicker or more extensive flows. However, there are currently few estimates of thickness for Venusian flows; some have been estimated to be 56 m to several hundred meters thick [*Moore and Schenk*, 1992], although these flows are believed to be more silicic (due to their ridged surface morphologies) than the flows we have considered here. The smooth surfaces and extensive nature of the flows associated with the polygonal patterns are more indicative of a basaltic composition such as that measured by five of the Soviet Venera landers [*Basilevsky and Surkov*, 1989]. A mechanism which could result in a relationship between joint spacing and lava flow thickness is described in studies on the propagation of tensional cracks in a brittle solid [*Nemat-Nasser et al.*, 1980; *Keer et al.*, 1978; *Nemat-Nasser et al.*, 1978]; we give a brief summary. For an initial crack configuration of parallel, equally spaced fractures of the same length and a conduction temperature profile, the fractures will grow until a critical state is reached. At this critical state, every alternate crack will stop growing and snap shut, and the remaining cracks will continue to propagate, until a second similar critical state is reached and so on. In this way, a final fracture spacing is obtained which is greater than the initial spacing and is dependent on the thickness of the brittle layer (via the number of critical states reached). Calculation of the initial crack spacing in a cooling Venusian lava (by assuming a fraction of the thermoelastic energy is used to initiate a fracture) gives a value of the order of millimetres. Extrapolation of millimeter spacing to kilometer spacing is unlikely. Even if the flows considered are 100 m thick, the ratio of polygon width to flow thickness is of the order of 10. However, if the flows are comparable in thickness to terrestrial flood basalts, then this ratio is of the order of 100 and the width of the tensile cracks is likely to be greater than the thickness of the flow.

Extrapolation of typical terrestrial joint spacings of decimeters to those of 1-2 km for Venus by any of the above mechanisms seems improbable. Spacings of the order of kilometers are more compatible with deformation of a layer thicker than that typical of terrestrial (and presumably Venusian) lava flows. The isotropic nature of the Venusian polygonal patterns is a strong reason for invoking a thermal origin; we next consider the thermal stresses resulting from regional heating of the lithosphere and an increased thermal gradient. As noted earlier, many of the areas exhibiting polygonal networks are areas of extensive volcanism, often in the form of shield fields. It has been suggested by *Aubele et al.* [1992] that shield fields represent areas of anomalous melting. We consider a less drastic scenario in which the temperature gradient in the regions of polygonal patterns is elevated due to an increased heat flux at the base of the lithosphere; the lithosphere thins and thermal stresses develop. We assume that the lithosphere is free to relieve the depth integrated stress. Stresses develop in the lithosphere according to

$$\Delta\sigma_{xx}(z,t) = -\alpha * \frac{E}{1-\nu} * \Delta T(z,t) + \frac{1}{h_e}\int_0^{h_e} \alpha * \frac{E}{1-\nu} * \Delta T(z,t)dz \quad (2)$$

[*Boley and Weiner*, 1960; *Parmentier and Haxby*, 1986], where h_e is the thickness of the elastic lithosphere. Other variables are as defined previously and tensional stresses are positive. For an increased temperature gradient and assuming linear geotherms before and after the lithosphere is heated, equation (2) reduces to

$$\Delta \sigma_{xx}(z,t) = \alpha * \frac{E}{1-\nu} * (c_2 - c_1) * \left(\frac{h_e}{2} - z\right) \quad (3)$$

where c_1 and c_2 are the original and elevated temperature gradients, respectively. Compressional stresses develop in the lower half of the thinned lithosphere and tensional stresses in the upper half. This process is shown schematically in Figure 6.

To investigate the failure associated with lithospheric thinning we compare the thermoelastic stresses (equation (2)) with a yield strength envelope model of the Venusian lithosphere. Without a good knowledge of lithospheric rheology on Venus, one can only adopt characteristic values used for the Earth's oceanic lithosphere [*Goetze and Evans*, 1979]. Here we follow *Solomon and Head* [1990] where they characterized the strength of the upper brittle portion of the lithosphere using a frictional sliding law [*Byerlee*, 1978] and the strength of the lower lithosphere using a ductile flow law for dry olivine (10^{-16} s^{-1} strain rate). These two failure criterion define a yield strength envelope (YSE) [*Goetze and Evans*, 1979] where the base of the YSE is approximately defined by the 740°K isotherm [*McAdoo et al.*, 1985]. Thus a higher-temperature gradient results in a weaker, thinner lithosphere.

As an example we consider a 25-km-thick lithosphere, which is the mean mechanical thickness derived from modeling of flexure at Nightingale Corona [*Johnson and Sandwell*, 1992]. The base of the elastic lithosphere is defined by the 740°C isotherm, so the resulting average temperature gradient at Nightingale is ~11°/km. Figure 7 shows the stress profiles obtained from (3) when the temperature gradient is elevated to 12°/km, 14°/km and 22°/km, representing increasing amounts of reheating and lithospheric thinning. In all cases the upper half of the thinned lithosphere is in tension and the lower half in compression. The maximum tensile stress, which occurs at z = 0, increases with increasing lithospheric thinning. The yield strength envelope (YSE) for dry olivine [*Kirby and Kronenberg*, 1987] for the elevated temperature gradient is also plotted. Brittle failure (dashed line) is assumed in the upper lithosphere [*Byerlee*, 1978]; this is independent of temperature gradient. Ductile flow (dotted line) is assumed in the lower lithosphere. The effect of increasing temperature gradient on the thickness and strength of the lower lithosphere can clearly be seen. Failure by ductile flow begins at increasingly shallower depths as the temperature gradient increases and the net strength of the lithosphere in both compression and tension (area within the YSE) also decreases. In this model we are not interested in what happens beneath the base of the thinned elastic lithosphere so the ductile flow part of the YSE is not considered further.

Brittle failure in the upper lithosphere will occur wherever the thermal stress given by (3) exceeds the yield strength, given by

$$S_t = 0.8 * \rho\, g\, z \quad (4)$$

[*Byerlee*, 1968; *Kirby*, 1983]. It can be seen from Figure 7 that the maximum depth to which failure will occur increases with the elevation in temperature gradient. In the case of linear geotherms there is a simple analytical solution for this depth. Equating (3) and (4) gives the maximum depth of failure as a function of the thickness of the thinned lithosphere h_e and temperature gradient increase (c_2-c_1):

$$z_{max} = \frac{47\,(c_2 - c_1)\,h_e}{(1.99 + 93\,(c_2 - c_1))} \quad (5)$$

We used a value of 8.86 m s^{-2} for g and 2800 kg m^{-3} for ρ. For the three degrees of thinning 12°/km, 14°/km, and 22°/km the maximum depth to which tensile failure will occur is 0.52 km, 1.2 km, and 2.1 km, respectively. The elevated temperature gradient of 14°/km would seem reasonable, predicting tensile failure of the upper 1.2 km of the lithosphere.

In the heated lithosphere model the crack width is much less than the thickness of the deformed layer. At Nightingale Corona if we take the range of polygon widths as 1-8 km and the range in the thickness of the deformed layer as 0.5-2 km (depending on the amount of reheating), we can get a crude estimate of the range in the ratio of polygon width to thickness of the deformed layer. This ratio varies from 0.5 to 16. It is interesting to note that this ratio is of the same order of magnitude as the ratio of wavlength of (dominant mode of) deformation to layer thickness in studies of deformation of thin layers under uniaxial compression/tension

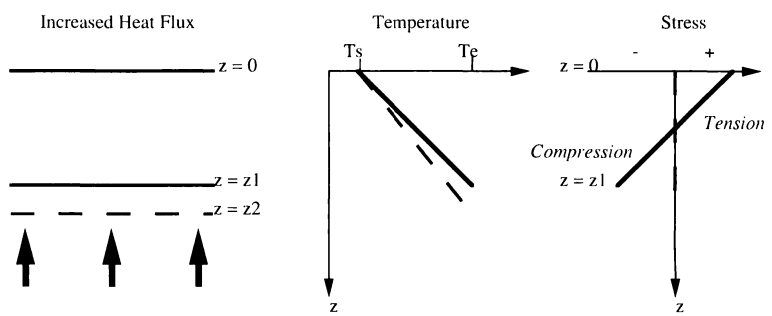

Fig. 6. Schematic representation of the development of thermal stresses in the lithosphere as a result of an increased temperature gradient. (*a*) Increased heat flux thins the lithosphere, (*b*) the temperature gradient (assumed linear) increases and thermal stresses develop. (*c*) The lithosphere is assumed to relieve the depth integrated stress, so tensional stresses result at the surface and compresssional stresses at depth as shown in the stress profile .

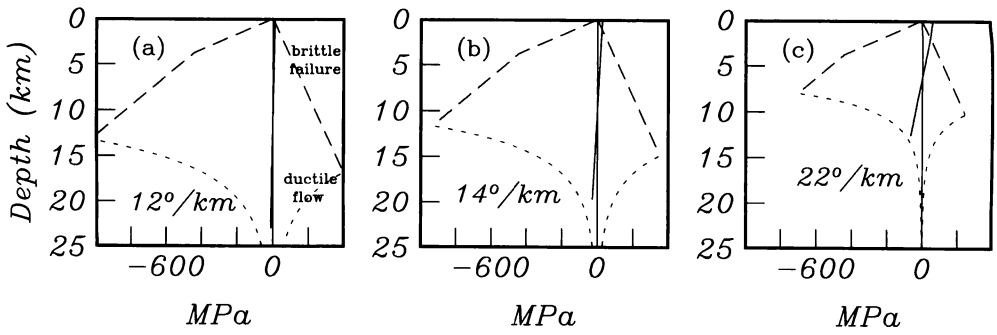

Fig. 7. Stress profiles and yield strength envelopes (for a dry olivine rheology) for elevation of the temperature gradient from 11°/km to (*a*) 12°/km, (*b*) 14°/km, (*c*) 22°/km. The dashed lines indicate the part of the YSE defined by brittle failure, the dotted lines indicate ductile flow. The stress profiles before (zero stress) and after the temperature gradient increase are shown as *solid* lines. Failure of the lithosphere occurs where the thermal stresses exceed the yield strength.

[*Ricard and Froidevaux*, 1986; *Zuber et al.*, 1986]. These studies predict that the deformation wavelength will be about 4 times the layer thickness.

The variation in spacing at Nightingale Corona is not explained by either the cooling flow or heated lithosphere scenario. However, in the heated lithosphere model the depth of failure is governed by the intensity of the increased heat flux, and so wider polygons could be the result of greater heating. This would imply a large lateral gradient in heat flow south of Nightingale Corona to account for the spatial variation in polygon size. Alternatively, the variation in polygon width may be related to the topographic flexure at Nightingale Corona. We have no quantitative explanation for this but the idea is supported by the observation that the wide polygons (> 3 km) are observed only at Nightingale Corona. In all other locations identified in Figure 1 the typical polygon widths are < 3 km, and in all these regions the topography is extremely flat.

CONCLUSIONS

The Venusian volcanic plains, as imaged by the Magellan spacecraft, show a wide range of tectonic and volcanic deformation patterns. We have considered a possible evolution for polygonal patterns identified in 15 regions. The polygonal patterns must arise as a result of an isotropic stress field, and we have proposed that they are tensional networks. The fractures defining the polygons have typical mean spacings of 1-2 km and widths at the resolution of the image pixels (75 m). Consideration of possible origins of an isotropic stress field in the volcanic plains leads to two possible scenarios. First, the patterns may be the result of residual thermal stress which would develop in a cooling lava flow. Residual tensional stresses which are much greater than the strength of unfractured terrestrial lava flows are predicted. The strain observed in the images is compatible with the thermal strain predicted only if the lineations defining the polygons are much less than 75 m wide. Second, the polygonal patterns may reflect deformation of a much thicker layer, such as brittle failure of the upper crust/lithosphere. A possible scenario involves an increased thermal gradient as a result of increased heat flux to the base of the lithosphere. Such an increase in heat flux is compatible with the evidence for extensive lava flows and shield fields in the regions exhibiting polygonal patterns. Assuming the lithosphere relieves the depth integrated stress, the increased temperature gradient predicts tensile stresses in the upper lithosphere and compressive stresses in the lower lithosphere. We have computed stress profiles for an initially 25-km-thick lithosphere with a temperature gradient of 11°/km by allowing the temperature gradient to increase to between 12°/km and 22°/km. The yield strength envelope for dry olivine corresponding to the increased temperature gradient was also computed. Brittle tensile failure occurs in the upper part of the lithosphere wherever the thermal stresses predicted exceed the yield strength. The maximum depth at which failure occurs increases with increasing elevation of the temperature gradient. In our numerical example this depth increased from 0.5 km for the temperature gradient of 12°/km to 2 km for the temperature gradient of 22°/km.

The cooling lava flow model can explain the existence, but not the scale, of isotropic patterns at the seven locations described in Table 1. This model requires that the limits of the polygonal patterns can be identified and correlated with individual flows. In most areas this is a difficult task due to later tectonic and volcanic events and the fact that the fractures defining some of the polygonal patterns are at the resolution of the radar. The heated lithosphere model does not require the same correlation of flows and polygonal patterns and so could account for all the areas identified in Figure 1. Neither model predicts the polygon widths or explains the variation in the polygonal patterns at Nightingale Corona. However, it is worth noting at this point that there is still progress to be made in our understanding of the evolution of joints in terrestrial columnar basalts, especially in explaining the final widths of the columns. Modeling of any kind of surface deformation on Venus would be aided greatly by better knowledge of the typical lithospheric thickness and strength and of the thermomechanical properties of lavas under Venusian conditions.

Acknowledgments. We gratefully acknowledge Steve Saunders and the Magellan Science team at JPL for making available the SAR images. Peter Ford and Gordon Pettengill (MIT) supplied the topography data. We also thank Chris Small for many helpful discussions and careful review of the manuscript. Noam Izenberg, Bob Brackett, Maya Tolstoy, Jim Happer, Walter Smith, and Si Nemat-Nasser provided helpful comments and suggestions. In addition, we acknowledge two anonymous reviewers. This work was completed under NASA contract JPL 958950.

REFERENCES

Aubele, J. C., L. S. Crumpler, and J. W. Head, Venus shield fields: Characteristics and implications, *Eos Trans. AGU, 73*, 178, 1992.

Aydin, A., and J. M. DeGraff, Evolution of polygonal fracture patterns in lava flows, *Science, 239*, 471-476, 1988.

Basilevsky, A. T., and Y. A. Surkov, Chemical composition of Venusian rocks and some geochemical implications, *Magellan project V Gram, Jet Propulsion Laboratroy, 15*, 2-4, 1989.

Boley, B. A., and J. H. Weiner, *Theory of Thermal Stresses*, John Wiley, New York, 1960.

Byerlee, J. D., Friction of rocks, *Pure Appl. Geophys.*, *116*, 615-626, 1978.

DeGraff, J. M., and A. Aydin, Dependence of columnar joint spacing and growth increment on cooling rate in lava flows, *Eos Trans. AGU*, *67*, 1211, 1986.

DeGraff, J. M., and A. Aydin, Surface morphology of columnar joints and its significance to mechanics and direction of joint growth, *Geol. Soc. Am. Bull.*, *99*, 605-617, 1987.

Ford, P. G., and G. H. Pettengill, Venus topography and kilometer-scale slopes, *J. Geophys. Res.*, this issue.

Goetze, C., and B. Evans, Stress and temperature in the bending lithosphere as constrained by experimental rock mechanics, *Geophys. J. R. Astron. Soc.*, *59*, 463-478, 1979.

Guest, J. E., and M. H. Bulmer, Volcanic edifices and volcanism in the plains of Venus, *Eos Trans. AGU*, *73*, 178, 1992.

Head, J. W., and L. Wilson, Volcanic processes and landforms on Venus: Theory, predictions and observations, *J. Geophys. Res.*, *91*, 9407-9446, 1986.

Head, J. W., and L. Wilson, Magma reservoirs and neutral buoyancy zones on Venus: Implications for the formation and evolution of volcanic landforms, *J. Geophys. Res.*, *97*, 3877-3903, 1992.

James, A. V. G., Factors producing columnar structure in lavas and its occurrence near Melbourne, Australia, *J. Geol.*, *28*, 458-469, 1920.

Johnson, C. L., and D. T. Sandwell, Flexure on Venus: Implications for lithospheric elastic thickness and strength, *Lunar Plant. Sci. Conf.*, *XXIII*, 619-620, 1992.

Keer, L. M., S. Nemat-Nasser, and A. Oranratnachai, Unstable growth of thermally induced interacting cracks in brittle solids: Further results, *Int. J. Solids Struc.*, *15*, 111-126, 1978.

Kirby, S. H., Rheology of the Lithosphere, *Rev. Geophys.*, *21*, 1458-1487, 1983.

Kirby, S. H., and A. K. Kronenberg, Rheology of the lithosphere: Selected topics, *Rev. Geophys.*, *25*, 1219-1244, 1987.

Long, P. E., and B. J. Wood, Structures, textures, and cooling histories of Columbia River basalt flows, *Geol. Soc. Am. Bull.*, *97*, 1144-1155, 1986.

McAdoo, D. C., C. F. Martin, and S. Poulouse, Seasat observations of flexure: Evidence for a strong lithosphere, *Tectonophysics*, *116*, 209-222, 1985.

Moore, H. J., and P. Schenk, Thick Lava Flows on Venus: Distribution, morphology and terrestrial comparisons, *Eos Trans. AGU*, *73*, 179, 1992.

Nemat-Nasser, S., L. M. Keer, and K. S. Parihar, Unstable growth of thermally induced interacting cracks in brittle solids, *Int. J. Solids Struc.*, *14*, 409-430, 1978.

Nemat-Nasser, S., Y. Sumi, and L. M. Keer, Unstable growth of tension cracks in brittle solids: Stable and unstable bifurcations, snap-through, and imperfection sensitivity, *Int. J. Solids Struc.*, *16*, 1017-1035, 1980.

Parmentier, E. M., and W. F. Haxby, Thermal stresses in the oceanic lithosphere: Evidence from geoid anomalies at fracture zones, *J. Geophys. Res.*, *91*, 7193-7204, 1986.

Peck, D. L., and T. Minakami, The formation of columnar joints in the upper part of Kilauean lava lakes, Hawaii, *Geol. Soc. Am. Bull.*, *79*, 1151-1166, 1968.

Pollard, D. P., and A. Aydin, Progress in understanding jointing over the past century, *Geol.Soc.Am. Bull.*, *100*, 1181-1204, 1988.

Ricard, Y., and C. Froidevaux, Stretching instabilities and lithospheric boudinage, *J. Geophys. Res.*, *91*, 8314-8324, 1986.

Ryan, M. P., and C. G. Sammis, Cyclic fracture mechanisms in cooling basalt, *Geol. Soc. Am. Bull*, *89*, 1295-1308, 1978.

Sabins, F. F., *Remote Sensing Principles and Interpretation*, W. H. Freeman, New York, 1978.

Saunders, R. S., R. E. Arvidson, J. W. Head, G. G. Schaber, E. R. Stofan, and S. C. Solomon, An overview of Venus geology, *Science*, *252*, 249-252, 1991.

Solomon, S. C., and J. W. Head, Lithospheric flexure beneath the Freyja Montes foredeep, Venus: Constraints on lithospheric thermal gradient and heat flow, *Geophys. Res. Lett.*, *17*, 1393-1396, 1990.

Spry, A. H., The origin of columnar jointing, particularly in basalt flows, *Geol. Soc. Aust. J.*, *8*, 191-216, 1962.

Stofan, E. R., G. Sharpton, G. Schubert, G. Baer, D. L. Bindschadler, D. M. Janes, and S. W. Squyres, Global distribution and characteristics of coronae and related features on Venus: Implications for origin and relation to mantle processes, *J. Geophys. Res.*, this issue.

Zuber, M. T., E. M. Parmentier, and R. C. Fletcher, Extension of continental lithosphere: A model for two scales of Basin and Range deformation, *J. Geophys. Res.*, *91*, 4826-4838, 1986.

C. L. Johnson and D. T. Sandwell, Scripps Institution of Oceanography, Geological Research Division, University of California, San Diego, 9500 Gilman Drive, La Jolla, CA 92093-0220.

(Received September 13, 1991;
revised May 22, 1992;
accepted May 27, 1992.)